Carbohydrate Polymers 89 (2012) 571–577

Contents lists available at SciVerse ScienceDirect

Carbohydrate Polymers

journal homepage: www.elsevier.com/locate/carbpol

Physicochemical properties of rhizome starch from a traditional Chinese medicinal plant of *Anemone altaica*

Jianmin Man[a,b], Jinwen Cai[a,b], Canhui Cai[a,b], Huyin Huai[b,**], Cunxu Wei[a,b,*]

[a] Key Laboratories of Crop Genetics and Physiology of the Jiangsu Province and Plant Functional Genomics of the Ministry of Education, Yangzhou University, Yangzhou 225009, China
[b] College of Bioscience and Biotechnology, Yangzhou University, Yangzhou 225009, China

ARTICLE INFO

Article history:
Received 1 December 2011
Received in revised form 10 February 2012
Accepted 19 March 2012
Available online 28 March 2012

Keywords:
Anemone altaica
Rhizome
Starch
Morphology
Physicochemical properties

ABSTRACT

This study investigated the physicochemical properties of rhizome starch of *A. altaica* for the first time. The results were compared to those obtained from two common starches (potato and rice). The rhizome had a starch content of 49.8%. Isolated starch granules were mostly oval in shape with a central Maltese cross and an average long axis of 6.25 μm. The starch contained 35.5% amylose and had lower gelatinization and pasting temperatures than rice and potato starches and a swelling power comparable to potato. Altaica starch had high breakdown and setback viscosities. X-ray diffraction revealed B-type starch with relative degree of crystallinity of 17.5%. Starch possessed a high susceptibility to hydrolysis by acid, porcine pancreatic α-amylase and *Aspergillus niger* amyloglucosidase when compared with potato and rice starches.

1. Introduction

Anemone altaica Fisch. ex C. A. Mey, belonging to the family Ranunculaceae, is widespread throughout the north of Asia and Europe (The Editorial Board of Flora of China, 1980). The rhizomes of *A. altaica* are believed to have anti-inflammatory and analgesic properties and have been used in the treatment of epilepsia, neurasthenia, and arthritis in traditional Chinese medicine for a long time (Wu, Zhou, & Xiao, 1988). Previous studies on the chemical constituents of *A. altaica* lead to the isolation, purification and structure identification of some small-molecule active ingredients, such as anemonin, palmitic acid, succinic acid, isoferulic acid, cirsiumaldehyde, and carboxymethyl isoferulate (Zou & Yang, 2008; Zou, Dong, & Yang, 2005). However, the macromolecules such as starch contained in the rhizome of *A. altaica* and other medicinal plants have hardly been studied and are therefore not utilized (Wang, Gao, Chen, & Xiao, 2006). In order to make good use of traditional Chinese medicinal plant of *A. altaica* and widen its application, starch was isolated from the rhizome of *A. altaica*. The physicochemical properties of *A. altaica* starch were investigated for the first time.

2. Materials and methods

2.1. Plant material

The rhizome of *A. altaica* was collected from a valley (N34°18.209′, E106°33.507′, alt. about 1400 m) of Xiaolongshan Mountain in Tianshui, Gansu Province, in May, 2011. The tuber of potato (*Solanum tuberosum* L.) was purchased from a local natural food market (Yangzhou City, China). Mature grain of rice (*Oryza sativa* L.) cv. Teqing was obtained from Agricultural College of Yangzhou University and grown in the university experimental field, Yangzhou, China, during the growing season.

2.2. Starch content

Quantitative determination of starch contents in dry *A. altaica* rhizome and rice grain was carried out according to the colorimetric method of anthrone-H_2SO_4 (McCready, Guggolz, Silviera, & Owens, 1949). The experiments were performed in triplicate.

2.3. Isolation of native starches

Native starch granules were isolated following a method described by Wei, Qin, Zhu, et al. (2010) with a slight modification.

Abbreviations: AAG, *Aspergillus niger* amyloglucosidase; ATR-FTIR, attenuated total reflectance-Fourier transform infrared; DSC, differential scanning calorimetry; PPA, porcine pancreatic α-amylase; RVA, rapid visco analyzer; XRD, X-ray powder diffraction.

* Corresponding author at: College of Bioscience and Biotechnology, Yangzhou University, Yangzhou 225009, China. Tel.: +86 514 87997217.
** Corresponding author. Tel.: +86 514 87965553.
E-mail addresses: hyhuai@yzu.edu.cn (H. Huai), cxwei@yzu.edu.cn (C. Wei).

0144-8617/$ – see front matter © 2012 Elsevier Ltd. All rights reserved.
doi:10.1016/j.carbpol.2012.03.049

Briefly, the rhizome of *A. altaica* and the tuber of potato were sliced into small pieces. The rice grains were steeped in double-distilled water at 4 °C for 16 h. The rhizome and tuber pieces and softened grains were homogenized with ice-cold water in a home blender. The homogenate was squeezed through four layers of cheesecloth by hand. The fibrous residue was homogenized and squeezed twice more with ice-cold water to facilitate the release of starch granules from the fibers. The combined extract was filtered with 100, 200, 300 and 400 mesh sieves and centrifuged at $3000 \times g$ for 10 min. The yellow gel-like layer on top of the packed white starch granule pellet was carefully scraped off and discarded. The process of centrifugation separation was repeated several times until no dirty material existed. The white starch sediment was further washed with anhydrous ethanol, dried at 40 °C, ground into powders, and passed through a 100-mesh sieve.

2.4. Morphology observation of starches

A starch suspension (1%, w/v) was prepared with 50% glycerol. A small drop of starch suspension was placed on the microscope slide and covered with a coverslip. The starch granule shape and Maltese cross were viewed with an Olympus BX53 polarized light microscope equipped with a CCD camera.

2.5. Particle size analysis of starches

The sizes of starch granules were analyzed. Images of starch granules were analyzed using JEDA-801D morphological image analysis system (Jiangsu JEDA Science-Technology Development Co., Ltd., Nanjing, China). More than 1 000 starch granules were analyzed per sample. Starch granules were grouped according to the long axis length, and the number of starch granules in each group was counted. Plotting the relative number of starch granules against the long axis length produced a starch granule size-distribution curve.

2.6. Amylose content determination

Amylose content of starches was determined using the iodine adsorption method of Konik-Rose et al. (2007) with some modifications. About 10 mg of starch was weighed (accurate to 0.1 mg) into a 10 ml screwcapped tube, then dissolved in 5 ml of urea dimethyl sulfoxide (UDMSO) solution. Dissolution was obtained by incubating the mixture at 95 °C for 1 h with intermittent vortexing. A 1 ml aliquot of the starch-UDMSO solution was treated with 1 ml of iodine solution (0.2% I_2 and 2% KI, w/v) and made up to 50 ml with water. The solution was immediately mixed and placed in darkness for 20 min. Apparent amylose content was evaluated from absorbance at 620 nm. The recorded values were converted to percent of amylose by reference to a standard curve prepared with amylose from potato (Sigma–Aldrich A-0512) and amylopectin from corn (Sigma–Aldrich 10120). The experiments were performed in triplicate.

2.7. Thermal property of starches

Thermal property of starches was measured using a differential scanning calorimetry (DSC) (200-F3, NETZSCH, Germany) as described previously by Wei et al. (2011). Starch (~5 mg, dry starch basis) was precisely weighed and mixed with 3 times (by weight) deionized-distilled water (~15 μl). The mixture was sealed in an aluminum pan overnight at 4 °C. After equilibrating for 1 h at room temperature, the starch sample was then heated from 25 to 110 °C at a rate of 10 °C/min. The experiments were performed in duplicate.

2.8. Swelling power determination of starches

Swelling power of starches was determined by heating starch-water slurries in a water bath at temperatures ranging from 40 to 95 °C in 5 °C intervals according to the procedures of Wei et al. (2011). The swelling power determination was performed in triplicate.

2.9. Pasting property of starches

The pasting property of starches (8% solids) was evaluated in triplicate with a Rapid Visco Analyzer (RVA-3D, Newport Scientific, Narrabeen, Australia). A programmed heating and cooling cycle was used, where the samples were held at 50 °C for 1 min, heated to 95 °C at a rate of 12 °C/min, maintained at 95 °C for 2.5 min, cooled to 50 °C at a rate of 12 °C/min, and then held at 50 °C for 1.4 min. Parameters recorded were pasting temperature, peak viscosity, hot viscosity, final viscosity, breakdown viscosity (peak-hot viscosity) and setback viscosity (final-hot viscosity).

2.10. Crystal structure analysis of starches

Crystal structure of starches was analyzed on an X-ray powder diffraction (XRD) (D8, Bruker, Germany) spectroscope. The XRD analysis and determination of the relative degree of crystallinity (%) of the starches were carried out following the method described by Wei, Qin, Zhou, et al. (2010). Before measurements, all the specimens were stored in a dessicator where a saturated solution of NaCl maintained a constant humidity atmosphere (relative humidity = 75%) for 1 week.

2.11. Structural order of starch external region

Ordered structure of starch external region was analyzed on a Varian 7 000 Fourier transform infrared (FTIR) spectrometer with a DTGS detector equipped with an attenuated total reflectance (ATR) single reflectance cell containing a germanium crystal (45° incidence-angle) (PIKE Technologies, USA) as previously described by Wei, Xu, et al. (2010). Original spectra were corrected by subtraction of the baseline in the region from 1200 to 800 cm^{-1} before deconvolution was applied using Resolutions Pro. The assumed line shape was Lorentzian with a half-width of 19 cm^{-1} and a resolution enhancement factor of 1.9. Intensity measurements at 1047, 1022, and 995 cm^{-1} were performed on the deconvoluted spectra by recording the height of the absorbance bands from the baseline using Adobe Photoshop 7.0 image software.

2.12. Hydrolysis of starch

Starches were hydrolyzed by porcine pancreatic α-amylase (EC 3.2.1.1) (PPA) (Sigma–Aldrich A-3176), *Aspergillus niger* amyloglucosidase (EC 3.2.1.3) (AAG) (Sigma–Aldrich A-7095) and HCl. The hydrolysis rates of starches by PPA and AAG were determined using the method of Li, Vasanthan, Hoover, & Rossnagel (2004) with some modifications. For PPA hydrolysis, isolated native starch (10 mg) was suspended in 2 ml of enzyme solution (0.1 M phosphate sodium buffer, pH 6.9, 25 mM NaCl, 5 mM $CaCl_2$, 0.02% NaN_3, 50 U PPA). For AAG hydrolysis, starch (10 mg) was suspended in 2 ml of enzyme solution (0.05 M acetate buffer, pH 4.5, 5 U AAG). The hydrolyses of PPA and AAG were conducted in a constant temperature shaking water bath with continuous shaking (100 rpm) at 37 and 55 °C, respectively, for 1, 2, 4, 8, 12, 24, 48, and 72 h.

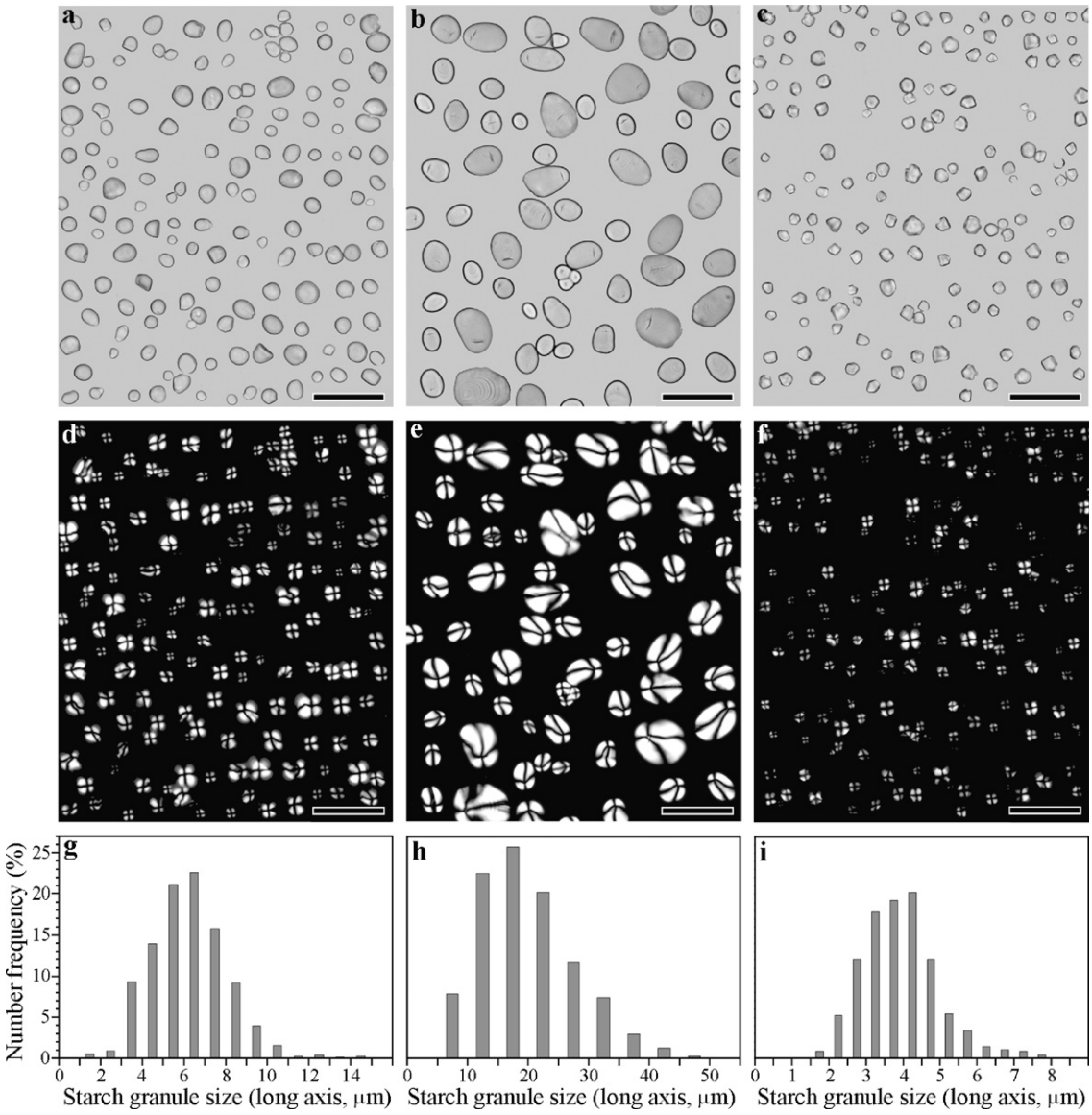

Fig. 1. Morphology and size-distribution of starches (a, d, g): *A. altaica* starch; (b, e, h): potato starch. (c, f, i): rice starch. (a–c): Light microscope graphs; (d–f): polarized light microscope graphs; (g–i): size-distribution curve of starch granules. Scale bar = 20 μm for (a, c, d, f) and 50 μm for (b, e).

The hydrolysis rate of starches by HCl was analyzed using the method of Wei, Xu, et al. (2010) with minor modification. 20 mg starch was suspended in 2 ml of 2.2 M HCl and hydrolysis was conducted in a constant temperature shaking water bath with continuous shaking (100 rpm) at 35 °C for 0.5, 1, 2, 4, 6, 8, 10, 12, and 14 d. After hydrolysis, starch slurries were quickly centrifuged (3000 × *g*) at 4 °C for 10 min. The supernatant was used for measurement of the solubilized carbohydrates to quantify the degree of hydrolysis by the anthrone-H_2SO_4 method (Wei, Xu, et al., 2010). The hydrolysis experiments were performed in triplicate.

2.13. Statistical analysis

The data reported in all the tables were mean values and standard deviation. Analysis of variance (ANOVA) by Tukey's test ($P < 0.05$) was evaluated using the SPSS 16.0 Statistical Software Program.

3. Results and discussion

3.1. Starch content

The starch contents (% based on dry weight) of *A. altaica* rhizome were 49.8%, which was significantly lower than that of rice grain (82.7%).

3.2. Morphology and size distribution of starches

Photomicrographs of starches taken from light microscope and polarized light microscope are presented in Fig. 1. *A. altaica* starches mostly showed oval-shaped granules, some truncated starch granules were also observed (Fig. 1a). Potato starches were large and had oval morphology (Fig. 1b). Rice starches were angular and oval to polyhedral in shape (Fig. 1c). The typical Maltese crosses were in the central position of *A. altaica* and rice starches (Fig. 1d and f) and at one end of potato starch granule (Fig. 1e). The differences in granule morphology and hilum may be attributed to the biological

Table 1
Sizes of starch granules.

Starch	Long axis length (μm)[a]	Short axis length (μm)[a]	Long/short axis[a]
A. altaica	6.25 ± 1.80b	5.24 ± 1.48b	1.20 ± 0.15a
Potato	19.87 ± 7.89c	15.68 ± 5.14c	1.25 ± 0.17b
Rice	3.93 ± 1.03a	3.33 ± 0.85a	1.19 ± 0.14a

Values in the same column with different letters were significantly different ($P < 0.05$).
[a] Data were means ± standard deviations, $n > 1000$.

origin, biochemistry of the amyloplast and physiology of the plant (Sandhu, Singh, & Kaur, 2004).

Starch granule sizes are usually measured by electrozone, image analysis, or laser light-scattering analysis methods. Harrigan (1997) found that using image analysis to determine starch granule size could yield accurate and reproducible data. Therefore, in this study, image analysis was used to determine starch granule size distribution. Fig. 1g–i shows the plots of number percent of particles over a range of the long axis length. They all showed unimodal size distributions. The statistical analysis of particle size is shown in Table 1. The average particle size (the long axis length) was 6.25, 19.87 and 3.93 μm for *A. altaica* starch and two starches used as controls (potato and rice starch), respectively.

3.3. Amylose content of starches

The amylose content plays an important role in starch internal quality. The amylose contents of *A. altaica*, potato, and rice starches were determined in this study to reveal starch internal quality (Table 2). *A. altaica* and potato starches showed similar amylose content. Rice starch had the lowest amylose content.

3.4. Thermal property of starches

DSC measures and records the amount of heat involved in the starch gelatinization. The gelatinization property of starch is related to a variety of factors including the size, proportion and kind of crystalline organization, and ultrastructure of the starch granules (Lindeboom, Chang, & Tyler, 2004). Thermal properties of *A. altaica*, potato and rice starches were determined by using a DSC, and their thermal parameters are given in Table 2. *A. altaica* starch had the lowest gelatinization temperatures which suggested that less energy was required to initiate gelatinization. The highest values for gelatinization temperatures were recorded for rice starch whereas potato starch exhibited intermediate values between the other two sources (Table 2). The gelatinization enthalpy values of starches have been reported to be affected by factors such as granule shape and the relative degree of crystallinity. The enthalpy values observed for different starches were 11.9, 15.6 and 12.5 J/g for native *A. altaica*, potato and rice starches, respectively. The variations in gelatinization enthalpy can represent differences in bonding forces between the double helices that

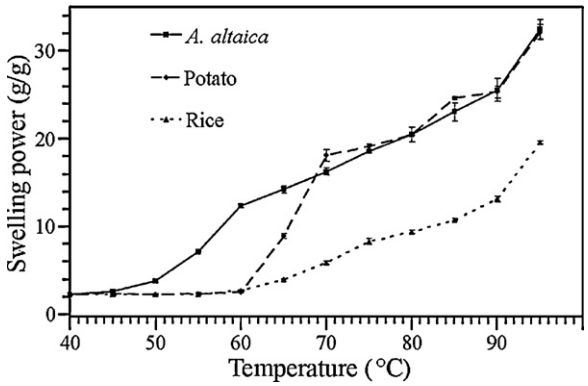

Fig. 2. Swelling powers of native starches.

form the amylopectin crystallites, which result in different alignment of hydrogen bonds within starch molecules (McPherson & Jane, 1999).

3.5. Swelling power of starches

According to starch gelatinization temperatures (Table 2), the swelling powers of *A. altaica*, potato and rice starches were investigated from 40 °C to 95 °C in 5 °C intervals (Fig. 2). Before gelatinization, swelling powers slightly increased with increasing temperature. After gelatinization, swelling power quickly increased. A sharp increase in swelling power of *A. altaica* starch was observed from 55 °C, while that in potato starch from 65 °C and in rice starch from 70 °C. Rice starch had a much lower swelling power throughout the range of temperatures (70–95 °C) compared with that of *A. altaica* and potato starches. Swelling power can be used to assess the extent of interaction between the starch chains, within the amorphous and crystalline of the starch granule. The swelling power of starch has been reported to depend upon the water holding capacity of starch molecules by hydrogen bonding. Hydrogen bonds stabilizing the structure of the double helices in crystallites are broken during gelatinization and are replaced by hydrogen bonds with water, and swelling is regulated by the crystallinity of the starch (Tester & Karkalas, 1996).

3.6. Pasting property of starches

Pasting properties of starches measured by using the RVA are summarized in Table 3. The RVA parameters of *A. altaica*, potato and rice starches were significantly different. Potato starch exhibited the highest peak and final viscosities followed by *A. altaica* and rice. Hot viscosity was highest in potato starch followed by rice and *A. altaica* starch. Breakdown and setback viscosities were observed to be highest in native *A. altaica* starch but lowest in native rice starch. The higher breakdown for *A. altaica* starch than potato and rice starches suggested that *A. altaica starch* was less resistant to heat and mechanical shear and hence more prone to loss viscosity

Table 2
Amylose contents and thermal properties of starches.

Starch	Amylose content (%)[a]	Thermal parameters[b]				
		T_o (°C)	T_p (°C)	T_c (°C)	ΔT (°C)	ΔH (J/g)
A. altaica	35.54 ± 0.52b	52.1 ± 0.1a	57.2 ± 0.1a	64.4 ± 0.2a	12.3 ± 0.2ab	11.9 ± 0.3a
Potato	34.71 ± 0.67b	64.3 ± 0.2b	69.0 ± 0.1b	77.0 ± 0.2b	12.7 ± 0.2b	15.6 ± 0.4b
Rice	27.32 ± 0.06a	72.4 ± 0.2c	78.1 ± 0.1c	83.8 ± 0.3c	11.4 ± 0.2a	12.5 ± 0.4a

Values in the same column with different letters were significantly different ($P < 0.05$).
[a] Data were means ± standard deviations, $n = 3$.
[b] T_o: onset temperature; T_p: peak temperature; T_c: conclusion temperature; ΔT: gelatinization range (T_c–T_o); ΔH: enthalpy of gelatinization. Data were means ± standard deviations, $n = 2$.

Table 3
Pasting properties of starches.

Starch	V_P (mPa s)	V_H (mPa s)	V_B (mPa s)	V_F (mPa s)	V_S (mPa s)	P_{Temp} (°C)
A. altaica	3824.3 ± 46.3b	2347.3 ± 12.5a	1477.0 ± 34.0c	3910.3 ± 3.4b	1563.0 ± 15.8c	62.7 ± 0.1a
Potato	5423.0 ± 55.5c	4433.0 ± 27.4c	990.0 ± 23.5b	5353.0 ± 36.5c	920.0 ± 8.7b	72.5 ± 0.0b
Rice	2833.7 ± 35.3a	2541.7 ± 33.1b	292.0 ± 2.9a	2845.0 ± 39.1a	303.3 ± 5.2a	81.3 ± 0.1c

V_P, peak viscosity; V_H, hot viscosity; V_B, breakdown viscosity, V_F, final viscosity, V_S, setback viscosity; P_{Temp}, pasting temperature.
Data were means ± standard deviations, $n = 3$. Values in the same column with different letters were significantly different ($P < 0.05$).

upon holding and shearing. The setback is the viscosity increase resulting from the rearrangement of amylose molecules that have leached from swollen starch granules during cooling, and is generally used as a measure of the gelling ability or retrogradation tendency of starch (Karim, Norziah, & Seow, 2000). The pasting temperature of *A. altaica* starch was the lowest (62.7 °C), whereas potato and rice starches had higher pasting temperatures (72.5 and 81.3 °C, respectively). The pasting properties of starches have been reported to be influenced by size, rigidity, amylose to amylopectin ratio and swelling power of the granules (Singh, Kaur, Ezekiel, & Guraya, 2005).

3.7. Crystallinity of starches

The XRD spectra of starches isolated from *A. altaica*, potato and rice are shown in Fig. 3. *A. altaica* and potato starches showed a typical B-type XRD pattern, while rice starch exhibited a typical A-type pattern (Fig. 3). In general, cereal grain starches give an A-type pattern, tuber and high-amylose cereal starches give a B-type pattern, and legume and *Dioscorea* rhizome starches present a C-type pattern (Cheetham & Tao, 1998; Wang, Yu, Yu, Chen, & Pang, 2007). The relative degrees of crystallinities of *A. altaica*, potato and rice starches calculated from the ratio of diffraction peak area and total diffraction area are given in Fig. 3. *A. altaica* starch showed the lowest relative degree of crystallinity, and potato starch had the highest relative degree of crystallinity.

3.8. Ordered structure of starch external region

The development of sampling devices like ATR-FTIR combined with procedures for spectrum deconvolution provides opportunities for the study of starch external region structure (Sevenou, Hill, Farhat, & Mitchell, 2002). The deconvoluted ATR-FTIR spectra in the region 1200–900 cm^{-1} of starches from *A. altaica*, potato and rice are presented in Fig. 4a. The bands at 1045 and 1022 cm^{-1} are linked with order/crystalline and amorphous regions in starch, respectively. The ratio of absorbance 1045/1022 cm^{-1} is used to quantify the degree of order in starch samples. Intensity ratios of 1045/1022 and 1022/995 cm^{-1} are useful as a convenient index of FTIR data in comparisons with other measures of starch conformation (Sevenou et al., 2002). The relative intensities of FTIR bands at 1045, 1022, and 995 cm^{-1} were recorded from the baseline to peak height, and the ratios for 1045/1022 and 1022/995 cm^{-1} were calculated (Fig. 4b).

On the basis of both the spectra and calculated data, *A. altaica*, potato and rice starches showed significantly different in the ratios of 1045/1022 and 1022/995 cm^{-1} (Fig. 4). Though FTIR is not able to differentiate starch crystal type. The starches with the same crystal type always show similar FTIR spectra, the band at 1022 cm^{-1} is more pronounced in A-type starch than in B-type or C-type starches (Sevenou et al., 2002). Our results showed that the IR ratio of 1045/1022 cm^{-1} was similar for *A. altaica* and rice starches, which was significantly lower than that of potato starch. The IR ratio of 1022/995 cm^{-1} was highest in rice starch.

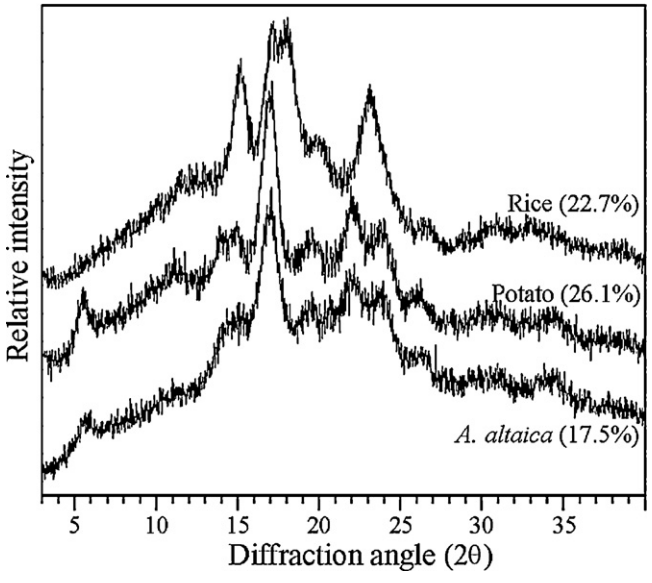

Fig. 3. XRD spectra of native starches. The relative degree of crystallinity (%) was given in parentheses.

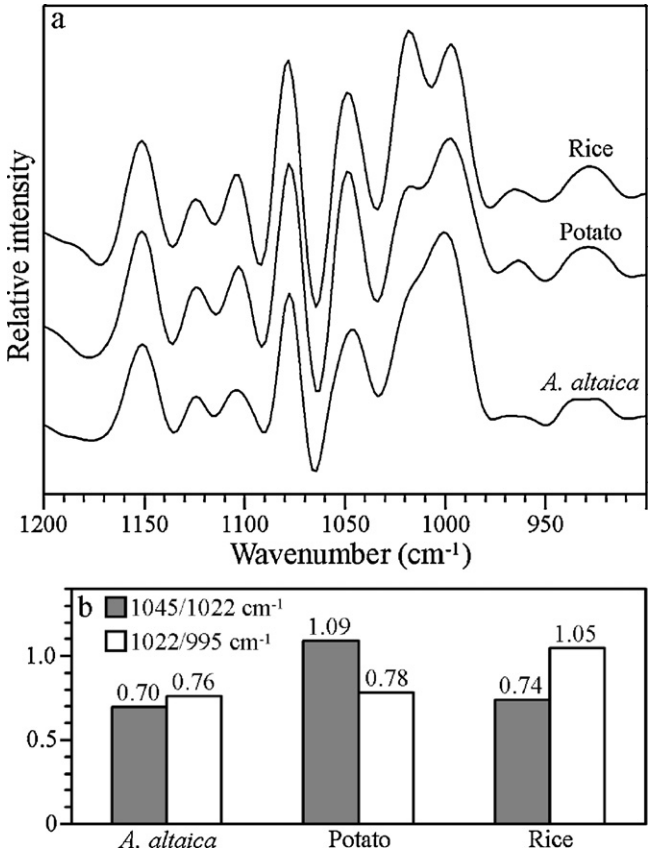

Fig. 4. Deconvoluted ATR-FTIR spectra (a) and IR ratio of absorbance (b) of native starches.

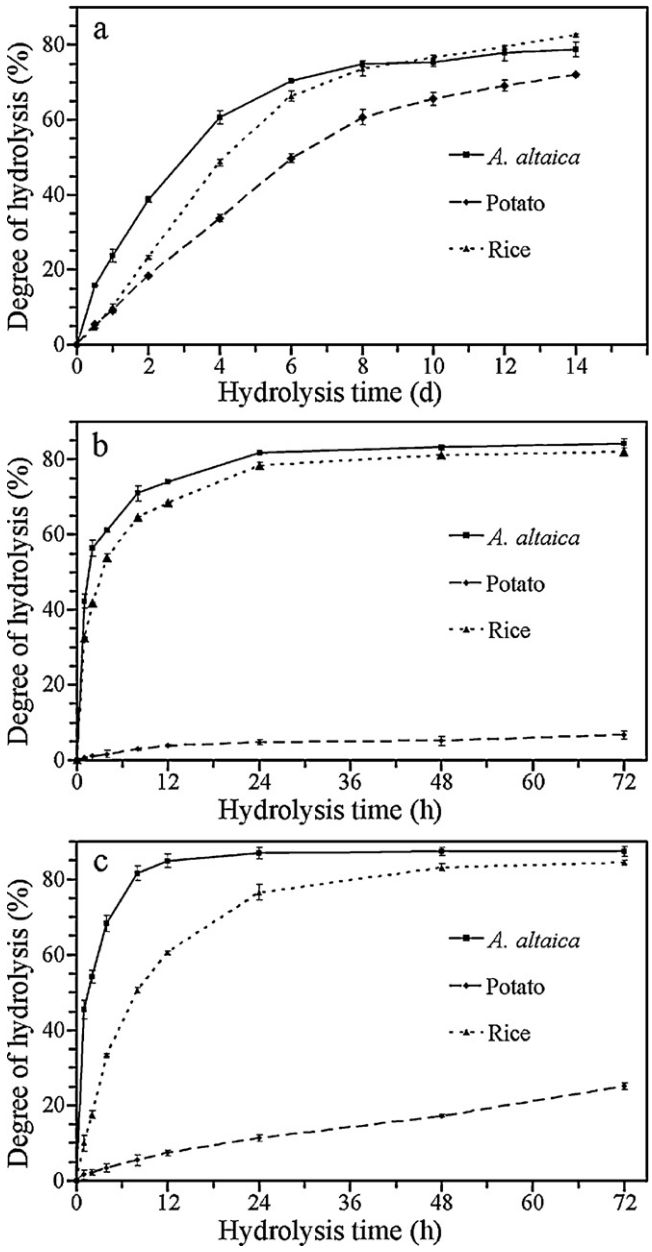

Fig. 5. Hydrolysis of starches by HCl (a), PPA (b) and AAG (c).

3.9. Hydrolysis property of starches

The hydrolysis degrees of *A. altaica*, potato and rice starches by HCl are presented in Fig. 5a. The hydrolysis degree increased gradually with increasing acid hydrolysis time. Two phases were distinguished in the acid hydrolysis of starch as a function of time. The initial rapid hydrolysis phase from 0 to 4 d for *A. altaica* starch, 0 to 6 d for rice starch, and 0 to 8 d for potato starch was mainly attributed to the hydrolysis of amorphous material. The later slower phase was to the hydrolysis of the crystalline region. Several hypotheses have been proposed for the protection of crystalline parts. First, hydronium ions are unable to penetrate the highly dense packing of double helices within the starch crystallites. Second, a high activation energy is required for a conformation change in glucose unit from a chair to a half-chair in order to be hydrolyzed (Srichuwong, Isono, Mishima, & Hisamatsu, 2005). The amorphous areas of the starch granules have a looser structure than the crystalline regions which are easier to attack with the hydronium ions. Native starches have some flaws on the surface of the granules which can provide channels for the infiltration of hydronium ions. These hydronium ions primarily get to the amorphous areas and attack them (Wang & Wang, 2001). Susceptibility to acid degradation of the starch granules is found to depend on plant origin.

The time course of PPA hydrolysis of starches is presented in Fig. 5b. The hydrolysis was biphasic, a relatively rapid rate at the initial stage (0–12 h), followed by a progressively decreased rate thereafter. A biphasic α-amylase hydrolysis trend has also been observed in starches with an initial rapid hydrolysis of the amorphous region followed by a decreased hydrolysis (Zhou, Hoover, & Liu, 2004). *A. altaica* and rice starches had similar hydrolysis degree of PPA. Potato starch had a high resistance to PPA hydrolysis. After 72 h of hydrolysis, the extent of hydrolysis was only about 6.7% for potato starch, which was markedly lower than that of *A. altaica* starch (84.3%) and rice starch (82.1%) (Fig. 5b). The hydrolysis of starches by AAG was also biphasic, a relatively rapid hydrolysis of the amorphous region at the initial stage, followed by a progressively decreased rate thereafter (Fig. 5c). *A. altaica* and rice starches also showed similar hydrolysis rate by AAG, which was markedly higher than that of potato starch. Susceptibility of starch to PPA and AAG attack is influenced by factors such as amylose to amylopectin ratio, crystalline structure, particle size and relative surface area, granule integrity, porosity of granules, and structural inhomogeneities (Blazek & Copeland, 2010). According to the present results, we thought that B-type potato starch had higher crystallinity and ordered structure at external region, larger granule size than *A. altaica* and rice starches did, which led to higher resistance to PPA and AAG for potato starch. Compared with rice starch, *A. altaica* starch had higher amylose content and lower crystallinity, which led to similar resistance to PPA and AAG for rice and *A. altaica* starches though *A. altaica* starch was B-type crystallinity.

4. Conclusion

Native starch was isolated from *A. altaica* rhizome with starch content of 49.8%, and its physicochemical properties were investigated. Starch granules were mostly oval in shape with average long axis length of 6.25 μm, and had typical central Maltese crosses. Starch contained 35.5% amylose and had high swelling power and low gelatinization and pasting temperatures. Starch had high breakdown and setback viscosities. Starch exhibited a B-type crystallinity, and the relative degree of crystallinity was 17.5%. Starch showed low degree of order at starch external region, and possessed high hydrolysis degrees of acid, PPA and AAG.

Acknowledgments

This study was financially supported by grants from the National Natural Science Foundation of China (30970285) and the Priority Academic Program Development of Jiangsu Higher Education Institutions.

References

Blazek, J., & Copeland, L. (2010). Amylolysis of wheat starches. II. Degradation patterns of native starch granules with varying functional properties. *Journal of Cereal Science*, *52*, 295–302.

Cheetham, N. W. H., & Tao, L. (1998). Variation in crystalline type with amylose content in maize starch granules: An X-ray powder diffraction study. *Carbohydrate Polymers*, *36*, 277–284.

Harrigan, K. A. (1997). Particle size analysis using automated image analysis. *Cereal Foods World*, *42*, 30–35.

Karim, A. A., Norziah, M. H., & Seow, C. C. (2000). Methods for the study of starch retrogradation. *Food Chemistry*, *71*, 9–36.

Konik-Rose, C., Thistleton, J., Chanvrier, H., Tan, I., Halley, P., Gidley, M., et al. (2007). Effects of starch synthase IIa gene dosage on grain protein and starch in endosperm of wheat. *Theoretical and Applied Genetics*, *115*, 1053–1065.

Li, J. H., Vasanthan, T., Hoover, R., & Rossnagel, B. G. (2004). Starch from hull-less barley: V. *In vitro* susceptibility of waxy, normal, and high-amylose starches towards hydrolysis by alpha-amylases and amyloglucosidase. *Food Chemistry*, *84*, 621–632.

Lindeboom, N., Chang, P. R., & Tyler, R. T. (2004). Analytical, biochemical and physicochemical aspects of starch granule size, with emphasis on small granule starches: A review. *Starch*, *56*, 89–99.

McCready, R. M., Guggolz, J., Silviera, V., & Owens, H. S. (1949). Determination of starch and amylose in vegetables. *Analytical Chemistry*, *22*, 1156–1158.

McPherson, A. E., & Jane, J. (1999). Comparison of waxy potato with other root and tuber starches. *Carbohydrate Polymers*, *40*, 57–70.

Sandhu, K. S., Singh, N., & Kaur, M. (2004). Characteristics of the different corn types and their grain fractions: Physicochemical, thermal, morphological and rheological properties of starches. *Journal of Food Engineering*, *64*, 119–127.

Sevenou, O., Hill, S. E., Farhat, I. A., & Mitchell, J. R. (2002). Organisation of the external region of the starch granule as determined by infrared spectroscopy. *International Journal of Biological Macromolecules*, *31*, 79–85.

Singh, N., Kaur, L., Ezekiel, R., & Guraya, H. S. (2005). Microstructural cooking and textural characteristics of potato (*Solanum tuberosum* L.) tubers in relation to physicochemical and functional properties of their flours. *Journal of the Science of Food and Agriculture*, *85*, 1275–1284.

Srichuwong, S., Isono, N., Mishima, T., & Hisamatsu, M. (2005). Structure of lintnerized starch in related to X-ray diffraction pattern and susceptibility to acid and enzyme hydrolysis of starch granules. *International Journal of Biological Macromolecules*, *37*, 115–121.

Tester, R. F., & Karkalas, J. (1996). Swelling and gelatinization of oat starches. *Cereal Chemistry*, *73*, 271–273.

The Editorial Board of Flora of China. (1980). *Flora of China* Beijing: Science Press., p. 12.

Wang, L. F., & Wang, Y. J. (2001). Structures and physicochemical properties of acid-thinned corn, potato and rice starches. *Starch*, *53*, 570–576.

Wang, S. J., Gao, W. Y., Chen, H. X., & Xiao, P. G. (2006). Studies on the morphological, thermal and crystalline properties of starches separated from medicinal plants. *Journal of Food Engineering*, *76*, 420–426.

Wang, S. J., Yu, J. L., Yu, J. G., Chen, H. X., & Pang, J. P. (2007). The effect of acid hydrolysis on morphological and crystalline properties of Rhizoma *Dioscorea* starch. *Food Hydrocolloids*, *21*, 1217–1222.

Wei, C. X., Qin, F. L., Zhou, W. D., Chen, Y. F., Xu, B., Wang, Y. P., et al. (2010). Formation of semi-compound C-type starch granule in high-amylose rice developed by antisense RNA inhibition of starch-branching enzyme. *Journal of Agricultural and Food Chemistry*, *58*, 11097–11104.

Wei, C. X., Qin, F. L., Zhu, L. J., Zhou, W. D., Chen, Y. F., Wang, Y. P., et al. (2010). Microstructure and ultrastructure of high-amylose rice resistant starch granules modified by antisense RNA inhibition of starch branching enzyme. *Journal of Agricultural and Food Chemistry*, *58*, 1224–1232.

Wei, C. X., Xu, B., Qin, F. L., Yu, H. G., Chen, C., Meng, X. L., et al. (2010). C-type starch from high-amylose rice resistant starch granules modified by antisense RNA inhibition of starch branching enzyme. *Journal of Agricultural and Food Chemistry*, *58*, 7383–7388.

Wei, C. X., Qin, F. L., Zhou, W. D., Xu, B., Chen, C., Chen, Y. F., et al. (2011). Comparison of the crystalline properties and structural changes of starches from high-amylose transgenic rice and its wild type during heating. *Food Chemistry*, *128*, 645–652.

Wu, Z. Y., Zhou, T. Y., & Xiao, P. G. (1988). *Compendium of Xinhua herbal book*. Shanghai: Science and Technology Publishing House.

Zhou, Y., Hoover, R., & Liu, Q. (2004). Relationship between α-amylase degradation and the structure and physicochemical properties of legume starches. *Carbohydrate Polymers*, *57*, 299–317.

Zou, Z. J., & Yang, J. S. (2008). Studies on the chemical constituents of the roots of *Anemone altaica*. *Journal of Chinese Medicinal Materials*, *31*, 49–51.

Zou, Z. J., Dong, Y. S., & Yang, J. S. (2005). Chemical constituents of the roots of *Anemone altaica* Fisch ex C. A. Mey. *Journal of Integrative Plant Biology*, *47*, 1145–1147.